Quantitative velocity modulation spectroscopy

James N. Hodges and Benjamin J. McCall

Citation: The Journal of Chemical Physics **144**, 184201 (2016); doi: 10.1063/1.4948740
View online: http://dx.doi.org/10.1063/1.4948740
View Table of Contents: http://scitation.aip.org/content/aip/journal/jcp/144/18?ver=pdfcov
Published by the AIP Publishing

Quantitative velocity modulation spectroscopy

James N. Hodges[1] and Benjamin J. McCall[1,2,a)]
[1]*Department of Chemistry, University of Illinois, Urbana, Illinois 61801, USA*
[2]*Departments of Physics and Astronomy, University of Illinois, Urbana, Illinois 61801, USA*

(Received 3 March 2016; accepted 22 April 2016; published online 13 May 2016)

Velocity Modulation Spectroscopy (VMS) is arguably the most important development in the 20th century for spectroscopic study of molecular ions. For decades, interpretation of VMS lineshapes has presented challenges due to the intrinsic covariance of fit parameters including velocity modulation amplitude, linewidth, and intensity. This limitation has stifled the growth of this technique into the quantitative realm. In this work, we show that subtle changes in the lineshape can be used to help address this complexity. This allows for determination of the linewidth, intensity relative to other transitions, velocity modulation amplitude, and electric field strength in the positive column of a glow discharge. Additionally, we explain the large homogeneous component of the linewidth that has been previously described. Using this component, the ion mobility can be determined. *Published by AIP Publishing.* [http://dx.doi.org/10.1063/1.4948740]

I. INTRODUCTION

The study of molecular ions poses several challenges to traditional direct absorption spectroscopy, such as low number density in glow discharges and large numbers of interfering neutrals. For 35 years, the gold standard for addressing these obstacles has been velocity modulation spectroscopy (VMS), which is a sensitive, ion-selective technique. Since its inception,[1] VMS has been used to study ~50 individual molecules[2] and has been enhanced by combination with heterodyne modulation, cavity enhancement, and direct frequency comb spectroscopy.[3–9] Despite the fact that VMS was developed in the infrared spectral region, it has seen extensive deployment in the millimeter/submillimeter wavelengths in support of rotational spectroscopy of molecular ions.[10–12]

The key to understanding ion selectivity in VMS is that the source responsible for generating the ions, the positive column of a glow discharge, is driven by an alternating electric field. As the polarity of the positive column changes, the ions experience a force that is proportional to the magnitude of the electric field and is along the axis of the discharge in the direction of the cathode. This ionic motion results in an oscillatory Doppler shift that can be detected by demodulation of the photo-signal with a phase sensitive detector, such as a lock-in amplifier. Under most conditions, the signals of neutrals are largely not affected by the electric field (the notable exception being processes involving excitation from charge transfer), so neutral signals can be filtered out at the demodulated frequency.[2] The demodulation scheme results in a derivative-like lineshape which makes it difficult to accurately determine linewidths, line strengths, and modulation depths (the ratio of the Doppler shift to the linewidth), as all these parameters are strongly correlated.

The theory of VMS lineshapes has been well established by John Farley in 1991.[13] The drift velocity (v) of ions in a positive column is directly proportional to the electric field magnitude (E), the proportionality constant being the ion mobility (K). The drift velocity of an ion in a static electric field is well known[14] and described in Equation (1)

$$v = KE. \tag{1}$$

The ion mobility depends on the temperature and pressure of the neutral collision partner, and it is often reported as a reduced ion mobility, K_0, adjusted to standard temperature and pressure. Because molecular collisions occur on the nanosecond time scale, whereas the period of the discharge is on the order of tens or hundreds of microseconds, we can assume that ions will rapidly achieve drift velocity,[13] because there are on the order of 10^3 to 10^4 collisions per half-cycle of the discharge. For experiments with a sinusoidal variation in electric field, there is, therefore, a sinusoidal variation in velocity such that

$$v(t) = KE\cos(2\pi t). \tag{2}$$

In this work we define the time (t) in fractional periods, a dimensionless quantity. This is a convenient choice as it avoids consideration of the driving frequency and any prefactors in the equations as a result of integration. The Doppler shift formula can be used to rewrite Equation (2) in frequency space,

$$\nu_{mod}(t) = v(t)\frac{\nu_0}{c} = \nu_{ma}\cos(2\pi t), \tag{3}$$

where $\nu_{mod}(t)$ is the time dependent transition frequency modulation in terms of ν_{ma}, the velocity modulation amplitude (VMA). The term, ν_0, is the center frequency of the transition. Over the course of the discharge cycle the line center changes as a function of time so the following transform must be applied to the spectroscopic lineshape (χ, a function of frequency detuning, ν) in order to model the

a)Electronic mail: bjmccall@illinois.edu. URL: http://bjm.scs.illinois.edu.

experiment

$$\chi(\nu) \rightarrow \chi(\nu + \nu_{mod}(t)). \tag{4}$$

Incidentally, this same transformation is used to model wavelength modulation lineshapes.[15] Velocity modulation and wavelength modulation are mathematically equivalent but differ in experimental realization. The former modulates the transition linecenter and the latter modulates the laser frequency. Wavelength modulation is sensitive to both ions and neutrals and lacks the ability to discriminate between the two, which is why VMS is preferentially used for molecular ion spectroscopy.

In most VMS experiments, there are two ion-related modulation processes that occur in tandem, and velocity modulation is not the only process that must be considered. Concentration modulation, the creation and destruction of ions during every half-cycle of the discharge, occurs at twice the frequency of the discharge. This is a challenging process to model *a priori*, but typically it has been assumed to follow the magnitude of the current sourced to the plasma. Generally, ion concentration increases with increased electron concentration,[13,16] so we assume a functional form for the ion concentration (ρ)

$$\rho(t) = \rho_0 |\cos(2\pi t)|, \tag{5}$$

where ρ_0 is the maximum ion concentration. This form is the same one previously used in other VMS works.[13,16]

The detected signal, the product of Equation (5) and the lineshape $\chi(\nu,t)$ as transformed by Equation (4), is demodulated by a lock-in amplifier, which may be considered a Fourier filter that selects only a single frequency component of the incoming signal. This is a multiplication of the signal by a reference signal and integration of the result over a period of the reference signal

$$\chi_{vms}(\nu) = \int_{-1/2}^{1/2} \rho(t)\chi(\nu,t)\cos(2\pi t + \phi)\, \mathrm{d}t. \tag{6}$$

Equation (6) describes the recorded lineshape, with an arbitrary phase, ϕ, which results in a maximum signal when velocity modulation is in-phase with the reference signal.

A proper fit of the VMS lineshape, though challenging due to the correlation of the width, intensity, and modulation depth, would allow for simultaneous determination of the electric field strength, the ion mobility, and the kinetic temperature of the spectral carrier. In cases where the carrier is unidentified, determination of the linewidth with sufficient precision could determine the mass of the carrier relative to the other species in the discharge, which has seen limited success in practice due to the problematic simultaneous determination of linewidth and VMA. Only large differences in mass were found to be reliable, such as the difference between one and two carbon atoms. As positive columns are rich chemical environments, mass identification by VMS is an untapped resource with many applications.

Presumably due to the difficulty of reliably determining covariant fit parameters, only two attempts to extract information from fits to VMS data have been made. The first was a study on ArH^+ and ArD^+ in 1994, wherein the lineshapes were integrated and fit to two overlapping Voigt profiles.[17] Although the results of that work are interesting, integration is not physically meaningful as VMS lineshapes are not the derivative of the underlying lineshape; rather, they are the time average of a function that oscillates in frequency and amplitude. In the second lineshape study by Gao *et al.*,[16] N_2^+ rovibronic transitions were fit with a Voigt profile as the fundamental lineshape, and they attributed the substantial homogeneous linewidth to pressure broadening. The primary limitation in that work is that the velocity modulation amplitude was held fixed to a theoretical value.

In this work, we present a computationally rapid method of separating the velocity modulation depth and the linewidth. The application of a pseudo-Voigt profile[18] is used as a reasonably accurate (~1%) and computationally trivial replacement to the full Voigt profile. Translational temperature assuming a known ionic mass, ion mobility, peak electric field strength, and line intensity is determined with low uncertainty. As VMS continues to be utilized in more complex techniques with additional layers of modulation,[4–6] a quantitative understanding of the fundamental VMS lineshape is crucial to successful fitting and analysis of more complicated data.

II. EXPERIMENT AND METHODOLOGY

A. Experiment

VMS experiments, though varied with specific light sources and detection scheme complexity, all are fundamentally the same type of experiment. Effectively, a laser passes through an AC modulated discharge cell and irradiates a detector. The output of that detector is read by a lock-in amplifier which is referenced to the discharge voltage. The output of the lock-in amplifier is then recorded as the frequency of the laser is tuned. A basic experiment is depicted in Fig. 1.

The molecule that is experimentally examined in this work is H_3^+. In this case, a continuous wave laser is single passed through a discharge cell and demodulated with a lock-in amplifier. For this work, a mid-IR optical parametric oscillator is used to scan the R(1,0) transition of the ν_2 fundamental band. Ions are generated in a liquid nitrogen cooled discharge of H_2 at a pressure of 500 mTorr. The cell has a central bore diameter of 18 mm.[19] The discharge is driven at 40 kHz by a ~4 kV peak-to-peak sinusoid. Frequency calibration

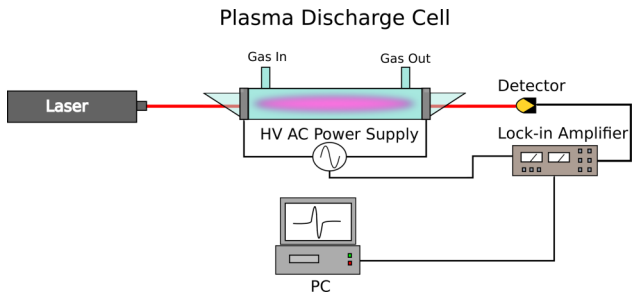

FIG. 1. A typical layout of a VMS spectrometer. It comprises a laser that spectroscopically probes a velocity modulated plasma. A detector converts the light into a voltage that is read by a lock-in amplifier, which is referenced to the voltage that drives the discharge.

is accomplished with a wavemeter (Bristol 621 IR-A) with a nominal uncertainty of 0.2 ppm. However, sub-optimal alignment results in less accurate readings. In the present work, the sole purpose of frequency calibration is to ensure a linear frequency axis as precision is more important to the contour of the lineshape than absolute frequency calibration. The light source, detector, and lock-in amplifiers used in the present work are described in detail in Crabtree *et al.*[20]

B. Method

As alluded to in Section I, the Voigt profile is required to adequately model the lineshape. Due to the fact that a nonlinear least squares routine makes multiple calls, and recognizing that numerical integration is part of the lineshape model, it is advantageous to have a computationally inexpensive form of the Voigt profile with which to work. Hence, we chose to use the pseudo-Voigt profile described in Thompson *et al.*[18]

The pseudo-Voigt profile (χ_{pV}) approximates the Voigt profile as a linear combination of Lorentzian and Gaussian transition profiles, given by Equation (7)[18]

$$\chi_{pV}(\nu;\nu_0,\Delta_V,\eta) = \eta L(\nu;\nu_0,\Delta_V) + (1-\eta)G(\nu;\nu_0,\Delta_V) \tag{7}$$

where

$$L(\nu;\nu_0,\Delta_V) = \frac{2\Delta_V}{\pi(4(\nu-\nu_0)^2+\Delta_V^2)} \tag{8}$$

and

$$G(\nu;\nu_0,\Delta_V) = \frac{2\sqrt{\ln 2}}{\Delta_V\sqrt{\pi}} e^{\frac{-(\nu-\nu_0)^2 4\ln 2}{\Delta_V^2}}. \tag{9}$$

The relevant parameters are the linear combination coefficient (η), the Voigt full-width at half-maximum (Δ_V), and the linecenter (ν_0). The η coefficient can be described in terms of the Lorentzian (Δ_L) and Voigt full-widths (Δ_V), and the Voigt full-width can be written in terms of the individual contributions to the full-width from the underlying Gaussian (Δ_G) and Lorentzian (Δ_L) profiles, which are the spectroscopically relevant parameters[18]

$$\Delta_V(\Delta_L,\Delta_G) = (\Delta_G^5 + 2.692\,69\Delta_G^4\Delta_L + 2.428\,43\Delta_G^3\Delta_L^2 + 4.471\,63\Delta_G^2\Delta_L^3 + 0.078\,42\Delta_G\Delta_L^4 + \Delta_L^5)^{\frac{1}{5}}, \tag{10}$$

$$\eta(\Delta_L,\Delta_V) = 1.366\,03(\frac{\Delta_L}{\Delta_V}) - 0.477\,19(\frac{\Delta_L}{\Delta_V})^2 + 0.111\,16(\frac{\Delta_L}{\Delta_V})^3. \tag{11}$$

This approximation has a maximum deviation of 1.2% at the center of the profile,[21] which contributes to the minimum relative uncertainty for any contour-based parameters extracted from the fit, i.e., terms that affect the actual lineshape such as width and velocity modulation amplitude. With a suitable expression for the fundamental lineshape (Equation (7)), the transform from Equation (4) is applied to cause the linecenter to oscillate in time with an amplitude of ν_{ma}, resulting in

$$\begin{aligned}\chi_{pV}(\nu,t;\nu_0,\Delta_V,\eta,\nu_{ma}) &= \eta L(\nu+\nu_{ma}\cos 2\pi t;\nu_0,\Delta_V)\\ &\quad + (1-\eta)G(\nu+\nu_{ma}\cos 2\pi t;\nu_0,\Delta_V).\end{aligned} \tag{12}$$

In order to arrive at a final functional form for integration, Equation (12) is multiplied by $\cos 2\pi t$ (selecting the frequency component equal to the driving frequency), multiplied by a transition intensity (A), and a y-offset (y_0) is added to account for a non-zero baseline. By integrating over a full discharge period, the final lineshape, χ_{vms}, is

$$\begin{aligned}\chi_{vms}(\nu;A,\nu_0,\Delta_L,\Delta_G,\nu_{ma},y_0) &= A\int_{-\frac{1}{2}}^{\frac{1}{2}} \chi_{pV}(\nu,t;\nu_0,\Delta_V(\Delta_L,\Delta_G),\eta(\Delta_L,\Delta_V),\nu_{ma})\\ &\quad\times\cos 2\pi t\,\mathrm{d}t + y_0.\end{aligned} \tag{13}$$

To summarize, the parameters from Equation (13) that are to be determined by the fit of Equation (13) to the experimental spectrum are the line intensity (A), linecenter (ν_0), homogeneous and inhomogeneous full-widths (Δ_L,Δ_V), velocity modulation amplitude (ν_{ma}), and y-offset (y_0).

In order to fit VMS lineshapes, a custom fitting program was written in `python3`, using the extensive `numpy` and `scipy` modules. The core functionality of the program is derived from the Levenberg-Marquardt nonlinear least squares routine from the `scipy.optimize` module. Integration is performed by the `numpy` module's `trapz` function, which is a trapezoidal rule numerical integration. The first step for integration is to define a two-dimensional array with frequency along one axis and time along the other. The size of the array is determined by a combination of the experimentally measured frequency data and the time step size that gives a sufficiently converged lineshape. Moreover, the number of time points is equal to the period divided by the step size, and the step size is chosen as a compromise between accuracy and integration time. Once the array is populated, the `trapz` function integrates along the time axis, which results in a one-dimensional array equivalent to the observed lineshape.

In order to determine a good step size, the integration was performed repeatedly with incrementally decreasing step size for a variety of different lineshape parameters. The integration time and the peak-to-peak intensity were recorded. Additionally, the standard deviation of the difference between the resultant lineshape with a given time step size and the lineshape of the previous step size are determined. In other words, after a new, smaller time step size is used for the integration, the new lineshape is differenced with the lineshape determined by a larger step size, and the standard deviation of the differences is recorded. This metric is useful as a measure of how much the line's contour changes from one time step size to the next smaller one.

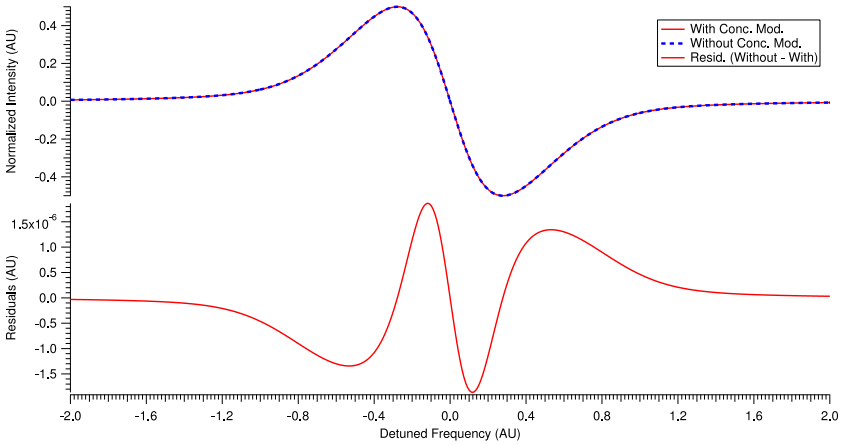

FIG. 2. Here, the effect of including concentration modulation versus ignoring it is highlighted. The overall peak-to-peak signal with concentration modulation is smaller than without it, so the signal for each was normalized to unity to illustrate errors in the contour. The residuals show some clear structure, though it is insignificant (~2 ppm) relative to other sources of error (~2%).

As a result of this convergence testing, a step size of 0.004 was chosen due to its reasonably quick integration time. The chosen step size exhibits less than 1% error as compared to the smallest time step (taken as the converged lineshape), 0.000 25 fractional periods. The 1% is the discrepancy between the peak-to-peak values of the chosen time step and the converged time step, and it is considered a contributing source of error to the contour of the lineshape.

Farley and Gao *et al.* include in their VMS models a term that accounts for concentration modulation, as described in Equation (5).[13,16] In tests we found that inclusion of Equation (5) does affect the absolute intensity; however, the overall effect on the contour is less than 2 ppm. As 2 ppm is far less than the error introduced by the pseudo-Voigt approximation and the numerical integration (~2% total), we have omitted concentration modulation from fits and simulations. Figure 2 illustrates the effect of including concentration modulation. The intensities were normalized to examine contour-based errors.

Fits of experimental data to Equation (13) with all parameters floating initially did not converge due to the large covariance between the velocity modulation amplitude (VMA) and full-width parameters. To circumvent this problem, the fit was performed first by holding the VMA constant at a value that corresponds to a rough estimate informed by the magnitude of the electric field and the ion mobility. The ion mobility can be approximated by the equation for the reduced ion mobility in Mason and McDaniel[14]

$$K_0 = \frac{13.876}{\sqrt{\alpha\mu}}. \tag{14}$$

The only necessary information is the polarizability of the neutral species (α in Å^3) and the reduced mass of the ion and its collision partner (μ in amu). The electric field strength can be approximated by dividing the applied voltage to the electrodes by the distance between the electrodes and reducing the result by an order of magnitude to account for the fact that most of the voltage drop in a glow discharge occurs in the space before the negative glow.[22] After the first fit converges, the residuals are examined for structure that indicates that the velocity modulation depth or VMD (ν_{ma}/Δ_V) is incorrect. The fixed VMA fit is performed several times to refine the VMA estimate, each time examining the residuals. When a good value for the VMA is determined, the fit is performed again floating all the parameters, and convergence is achieved. This approach works because the VMD has subtle effects on the central slope and extrema of the two lobes of VMS-type lines as summarized in Figures 3 and 4. As the VMD is increased, the interior of the extrema becomes more curved and the interior slope becomes less steep. The reason for these differences is that as the VMD is increased, the individual Doppler-shifted components become more resolved. For VMD < 10% it becomes more difficult to distinguish one value of VMD from another. Fits to data with low VMD are therefore likely prone to substantial error. The VMD determined from the fits to the data presented in this work is ~30%, which gives

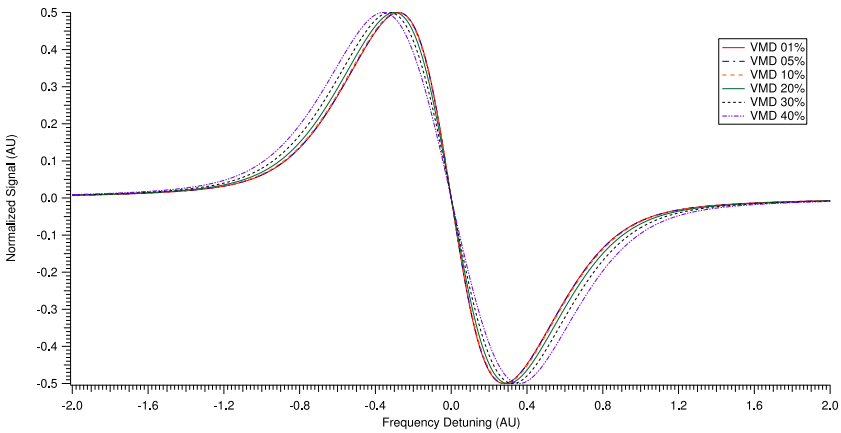

FIG. 3. The velocity modulation depth (VMD) has a subtle effect on the contour of VMS lineshapes. The peak-to-peak intensities of each lineshape are normalized to unity.

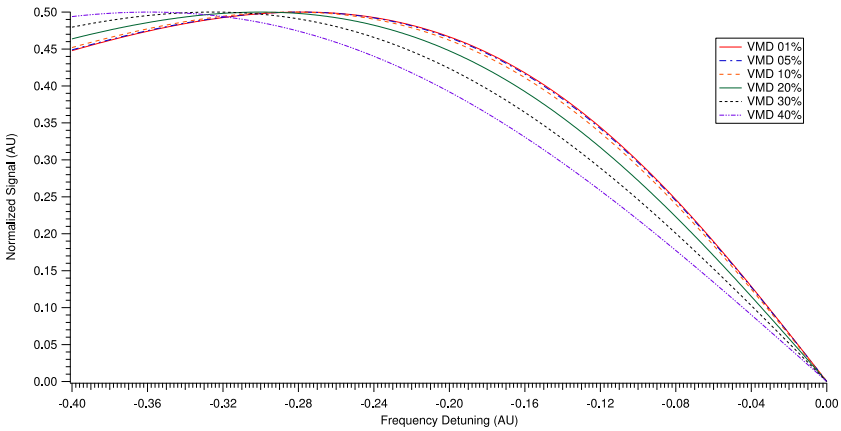

FIG. 4. Closer inspection of Figure 3 makes plain the effect of velocity modulation depth (VMD) on the lineshape.

confidence in the fitting approach. After the fit was converged, the value of the VMA can be substantially changed and the fit with the floating VMA will converge on the correct result.

III. RESULTS AND DISCUSSION

A single scan of the R(1,0) transition was recorded as described in Section II A. Using the method described in Section II B, a good fit was determined. The data, fit, and residuals can be seen in Figure 5, and a summary of the fitted parameters is presented in Table I.

The fitted parameters all exhibit extremely small uncertainties as reported by the least squares regression. In the case of the linecenter and y-offset these values can be taken as is, since they are not determined by the contour of the line and are not subject to the convergence error or the pseudo-Voigt approximation, which combined present the need for an additional 2% relative error to be added to the overall uncertainty of the remaining parameters (1% from the pseudo-Voigt approximation and 1% from the convergence error).

The intensity of the transition is sufficiently well determined as to present the opportunity for determining the relative populations of rovibrational levels. The absolute populations cannot be determined because concentration modulation has been excluded from the model. Under the assumption that the same concentration modulation uniformly affects each quantum state, relative determinations of populations are possible. Testing this hypothesis may provide for an interesting avenue of future investigation. Regardless of this limitation, more precise intensity will lead to more accurate rotational/vibrational temperature determination.

Another exciting prospect is that the relative uncertainty of the linecenter is sub-MHz. Though this work was performed with a wavemeter which has an appreciable accuracy error (~200 MHz), proper calibration with a frequency comb and careful control of the experimental conditions may allow this approach to rival the uncertainties determined by sub-Doppler techniques[5,6] without the added experimental difficulty. This would rely on the lines being very symmetric and highly reproducible, which may not always be the case. This problem could be mitigated with balanced detection of counter-propagating beams but would still be susceptible to any average drift velocity caused by asymmetries in the electrodes. This has been confirmed with these discharge electronics in the case of HCO^+, which exhibited between a 13 and 14 m/s average drift velocity.[23]

Both the inhomogeneous and homogeneous components of the linewidth were well determined. The two dominant broadening mechanisms for VMS spectroscopy are Doppler and collisional broadening. Plasmas are used for ion generation and result in large thermal energies. Typical VMS targets are low mass ions[2] which when combined with high temperatures result in mid-IR Doppler widths on the order of ~0.5 to ~1.0 GHz. The importance of collisional broadening is less obvious, considering a typical value for the

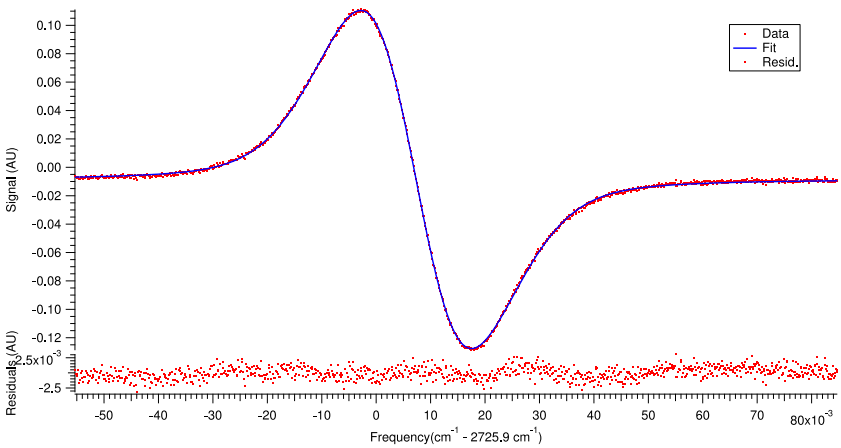

FIG. 5. Experimental spectrum and fit to the R(1,0) rovibrational transition in the ν_2 fundamental band of H_3^+. The standard deviation of the residuals is less than 1% of the peak-to-peak signal. The signal-to-noise ratio is ~240 which is very useful in determining the values accurately. There is some structure remaining in the residuals, but it is attributed to the negative lobe being slightly wider than the positive lobe, possibly as a result of an asymmetric drift velocity during half the discharge cycle.

TABLE I. Fit parameters from the R(1,0) transition of H_3^+.

Parameter	Symbol	Value	Error
Intensity	A	0.0220 V	0.0003 V
Linecenter	ν_0	2725.907 331 cm^{-1}	0.000 006 cm^{-1}[a]
Homogeneous linewidth	Δ_L	0.0140 cm^{-1}	0.0001 cm^{-1}
Inhomogeneous linewidth	Δ_G	0.0163 cm^{-1}	0.0001 cm^{-1}
Modulation amplitude	ν_{ma}	0.0079 cm^{-1}	0.0002 cm^{-1}
y-offset	y_0	−0.008 59 V	0.000 03 V

[a]This is not to suggest this is the total uncertainty of the transition frequency; rather, it is the uncertainty of the fit. This work is calibrated via a wavemeter, limiting the accuracy. For an accurate linecenter determination, see Hodges *et al.*[5]

pressure broadening coefficient is ∼1-10 MHz/Torr, and VMS spectroscopy is generally performed at pressures between 0.5 and 10 Torr. Nevertheless, Gao *et al.* showed that treating the lineshapes as completely inhomogeneously broadened is insufficient to describe the lineshape.[16] The magnitude of both these broadening mechanisms requires the use of a Voigt profile.

The Doppler width (Gaussian, Δ_G) is determined by the formula

$$\Delta_G = \sqrt{\frac{8kT\ln 2}{mc^2}} \tag{15}$$

and depends on the translational temperature (T) and mass (m) of the ion. The collisionally broadened full-width (Lorentzian, Δ_L) is inversely proportional to the mean time between phase-changing collisions (τ),

$$\Delta_L = \frac{1}{\pi\tau}. \tag{16}$$

To characterize the collisional process, we must consider the predominant collision partner for ions in a plasma. A typical fractional ionization is 10^{-4}, indicating that there are 10 000 more neutral molecules than ions or electrons in a plasma. Conventionally, the ion-ion and ion-electron collisions are neglected because the positive column is assumed to have zero net charge.[14] Higher order corrections for the non-uniform distribution of charge are generally neglected.[2] Therefore, the relevant collision partner is the more abundant neutral, and ion-neutral collisions are the principal type assumed in all VMS experiments.[2,13] Collisions of this type are typically described by Langevin capture theory, a simple model that has been successfully utilized to predict pressure broadening.[24]

The Langevin rate coefficient (k) is expressed in Equation (17) in terms of the polarizability of the neutral (α), the charge of the ion (q), and the reduced mass (μ) of the ion and its collision partner

$$k = 2\pi q\sqrt{\frac{\alpha}{\mu}}. \tag{17}$$

The relationship between the Langevin rate coefficient and the pressure broadening coefficient (γ), pressure (P), and mean time between collisions (τ) is given in Equation (18),[24]

$$\frac{1}{\tau} = nk = 2\pi\gamma P, \tag{18}$$

which can be combined with the ideal gas law and solved for the pressure broadening coefficient

$$\gamma = \frac{q\sqrt{\frac{\alpha}{\mu}}}{kT}. \tag{19}$$

This linewidth is a half-width value, so one would expect $\Delta_L = 2\gamma P$, resulting in a Δ_L on the order of tens of MHz, but Gao and coworkers required much larger values[16] as did the fits in the present work, indicating that Equation (19) is insufficient. Using the Langevin model, the expected homogeneous linewidth in Gao's experiment (N_2^+ at a pressure of 10 Torr) would be 26 MHz; however, Gao's reported homogeneous linewidth is much larger, on the order of the Gaussian linewidth. The collisional process must not be well described by the Langevin model, and there must be a different source for the homogeneous contribution to the linewidth.

In order to better understand the collisional environment that an ion in a positive column experiences, we must start from basic principles. Let us begin by considering the equation of motion for ions in an electric field, as described by Chen[25] and summarized by Civiš[17]

$$\mu\frac{\partial v}{\partial t} = qE - \frac{\mu}{\tau_D}v, \tag{20}$$

where the reduced mass of the ion and its collision partner is μ, v is the drift velocity, t is time, τ_D is the mean time between momentum transfer or diffusion related collisions, q is charge, and E is electric field strength. The first term on the right hand side is the force of the electric field on a charged particle, and the second term is analogous to a drag force linearly proportional to the speed of the charged particle. Solving this equation of motion by assuming a constant electric field gives

$$v(t) = \frac{q\tau_D}{\mu}E(1 - e^{-t/\tau_D}) + v_0e^{-t/\tau_D}, \tag{21}$$

where v_0e^{-t/τ_D} is a collisional deceleration term indicating that as time increases, the initial velocity is less significant. Likewise, as time increases the velocity approaches $\frac{q\tau_D}{\mu}E$.

Equation (21) is a complete description of an ion's speed, but it can be greatly simplified. Recall that the relationship between drift velocity (v), ion mobility (K), and electric field strength (E) is given by Equation (1). As the time scale of the discharge is many orders larger than the time scale of molecular collisions, the relevant time, t, is much greater than τ_D, and Equation (21) can be simplified to

$$v(t) \cong \frac{q\tau_D}{\mu}E. \tag{22}$$

Comparison of Equation (22) to Equation (1) reveals that the ion mobility is

$$K \cong \frac{q\tau_D}{\mu}, \tag{23}$$

which indicates that an estimate of the ion mobility can be made provided information about the mean time between momentum transfer collisions can be determined.

However, τ from Equation (16) and τ_D from Equation (22) are not equivalent. The value τ is related to an ion's collisional cross section ($\sigma(\bar{v})$) at a mean speed ($\bar{v}$) by $\tau = (n\bar{v}\sigma(\bar{v}))^{-1}$; whereas, τ_D is related to the momentum transfer/diffusional cross section (Q_D) by $\tau_D = (n\bar{v}Q_D)^{-1}$. Here n is the number density and $\bar{v}$ is the mean velocity. Both values of τ can be related through n and $\bar{v}$:

$$\tau_D = \frac{\sigma}{Q_D}\tau. \tag{24}$$

The definition of Q_D, as described by Mason and McDaniel,[14] is

$$Q_D \equiv 2\pi \int_0^{\pi} (1 - \cos\theta)\sigma(\theta, \bar{v}) \sin\theta \, d\theta, \tag{25}$$

where $\sigma(\theta, \bar{v})$ is the collisional cross section as a function of scattering angle, θ and mean relative speed of the ion, $\bar{v}$. Without detailed knowledge of the potential energy surface of a scattering event for a particular ion-neutral pair, it is impossible to determine $\sigma(\theta, \bar{v})$. For simplicity, we make the assumption that the cross section is only weakly dependent on the scattering angle such that $\sigma(\bar{v}) \approx \sigma(\theta, \bar{v})$. Using this assumption, Equation (25) becomes

$$Q_D \approx 2\pi\sigma \int_0^{\pi} (1 - \cos\theta) \sin\theta \, d\theta = 4\pi\sigma. \tag{26}$$

Combining Equations (24) and (26), an approximate relation for τ and τ_D can be formulated

$$\tau_D \cong \frac{\tau}{4\pi}. \tag{27}$$

This simple equation relates the spectroscopically observed linewidth from τ and Equation (16) to the ion mobility through τ_D and Equation (23). Simultaneously it provides an explanation of the large values of the homogeneous linewidth with a simple model derived from the equation of motion presented in Equation (20). The source of the homogeneous linewidth is the collisional enhancement due to the macroscopic motion of the ions in the plasma. As the electric field drives the ions, collisions with neutrals create a drag force balancing the electromagnetic force resulting in a fixed single velocity. The rate of these collisions is determined by the diffusional cross section, which ultimately determines an ion's mobility. This relationship allows us to express the homogeneous full-width in terms of the ion mobility by

$$\Delta_L = \frac{q}{4\pi^2 \, \mu \, K(T,p)}. \tag{28}$$

With a clear understanding of the homogeneous and inhomogeneous linewidths, the fitted values can be used to infer information about the physical conditions and molecule being spectroscopically interrogated. Application of Equation (15) results in a translational temperature of 209 ± 10 K. This is a reasonable temperature and is in accord with previous estimates (200-400 K) of the temperature of liquid nitrogen cooled discharges of molecular hydrogen.[19,26] As the inhomogeneous linewidth is also mass dependent, an analysis of many spectral lines could, in principle, be used to properly distinguish the relative masses of carriers, assuming a Maxwellian velocity distribution. In this case, the mass resolution is 0.03 amu, which is determined by propagating the linewidth error in Equation (15) using a fixed value for temperature. With such a small mass resolution, VMS could be a very powerful tool for distinguishing spectral carriers in chemically rich positive columns, which would be invaluable for assigning unknown spectra.

Using the homogeneous linewidth we can determine the ion mobility. The Langevin model linewidth is estimated using the temperature and the polarizability of molecular hydrogen (0.787 Å^3 ± 5%).[27] This results in a Langevin pressure broadened component equal to 14 ± 2 MHz. Just as in Gao's measurements of N_2^+, this is a dramatic underestimate. With Equation (16), τ is determined to be $7.8 \pm 0.3 \times 10^{-10}$ s. With Equation (27), the value of τ_D is calculated to be $6.0 \pm 0.2 \times 10^{-11}$ s. This can be used with Equation (23) to infer the ion mobility. The determination of reduced ion mobility assumes that the reading of the pressure capacitance monometer is accurate to 5%, and it is calculated to be 12.5 ± 1.5 cm^2 V^{-1} s^{-1} which agrees with the most recent literature value of 11.1 cm^2 V^{-1} s^{-1} within 13% error.[28]

In this case it is fortunate that there is a large signal-to-noise ratio and the VMD (~30%) is in a range that allows for reasonable determination of the VMA (refer to Figure 4). This may not be the case in all VMS experiments. Since the VMD is the ratio of the VMA to the linewidth there are only a limited number of experimental parameters that can be adjusted to ensure a large VMD. The temperature can be reduced and the pressure decreased to minimize the linewidth, and the applied voltage to the electrodes can be increased in order to increase the VMA. Nevertheless, the VMD may still prove too small for some systems. Moving forward, caution is required to properly determine the fitted parameters. Determination of fit parameters below a VMD of ~20% becomes more challenging and ultimately becomes an exercise in futility. This is a direct consequence of how insensitive the contour of the lineshape becomes to changes in VMD (refer to Figure 4).

The RMS value of the drift velocity (determined as 614 ± 16 m/s from Equation (4) and the VMA from the fit) can be used to determine the RMS field strength using Equation (1), provided the ion mobility is accurately known. Using the literature value, the RMS field strength is determined to be 4.8 ± 0.6 V/cm. If one were to take the applied voltage and divide it by the distance between the electrodes, the resultant RMS field strength would be 24 V/cm. Typically, the values in the positive column are an order of magnitude lower,[22] and our inferred field strength of 4.8 V/cm is in accord with that rough estimate. The calculated value of the ion mobility can be used in cases where the reduced ion mobility is not known. With this method, the RMS field strength is determined to be 4.2 ± 0.2 V/cm, which is in reasonable agreement with the other measurement.

IV. CONCLUSIONS

In this work, we present a method for quantitatively fitting VMS lineshapes. This method relies on a detailed examination of the slope of the center portion of the profile and the curvature near the edges of the lobes. Additionally, we confirm that there is a large homogeneous component to the linewidth of VMS greater than what can be explained by Langevin capture theory. This is attributed to the macroscopic movement of ions at the drift speed and the resulting collisional enhancement. From the fit, the translational temperature, transition intensity, ion mobility, and electric field strength are handily determined to reasonable uncertainty.

Together, these values are critical for the quantitative understanding of both the plasma environment and the species being interrogated spectroscopically. This may help lead to better quantification of relative ion populations, rotational and vibrational temperatures, mass identification of spectral carriers, and a better understanding of the lineshapes of more complicated VMS experiments with additional layers of modulation. As a final note, although this method is completely general to any VMS experiment, it does require high data quality and that the VMD be appreciably sized. As the VMD value becomes smaller the task becomes more challenging and requires higher signal-to-noise data.

So long as there is highly reproducible data with high signal-to-noise, it is expected that statistical errors, determined by scanning the same transition multiple times, will be on the same order as the estimated error of fitted parameters. This might be an interesting endeavor for future experiments. Additionally, this same analysis should be performed on different molecules to confirm the generality of this approach.

ACKNOWLEDGMENTS

We would like to acknowledge support from the National Science Foundation (Grant No. CHE 12-13811) and the NASA Laboratory Astrophysics program (Grant No. NNX13AE62G). J.N.H. is appreciative for the support from a Robert and Carolyn Springborn Fellowship and an NSF Graduate Research Fellowship (Grant No. DGE 11-44245 FLLW). J.N.H. is grateful to Adam J. Perry for his assistance in collecting data for the paper. J.N.H. is also appreciative to Thomas C. Allen for useful discussions regarding approaches to fast and accurate numerical integration, Charles R. Markus for useful discussions regarding the homogeneous broadening model, and Daniel N. Gresh for sharing his experimental data that was useful in demonstrating the necessity of high signal-to-noise ratios for the success of this approach. J.N.H. is also especially appreciative of Yahsin Chen for her hard work in translation of H. Gao's paper.

[1]C. Gudeman, M. Begemann, J. Pfaff, and R. Saykally, Phys. Rev. Lett. **50**, 727 (1983).
[2]S. K. Stephenson and R. J. Saykally, Chem. Rev. **105**, 3220 (2005).
[3]B. M. Siller, A. A. Mills, and B. J. McCall, Opt. Lett. **35**, 1266 (2010).
[4]B. M. Siller, M. W. Porambo, A. A. Mills, and B. J. McCall, Opt. Express **19**, 24822 (2011).
[5]J. N. Hodges, A. J. Perry, P. A. Jenkins II, B. M. Siller, and B. J. McCall, J. Chem. Phys. **139**, 164201 (2013).
[6]A. J. Perry, J. N. Hodges, C. R. Markus, G. S. Kocheril, and B. J. McCall, J. Chem. Phys. **141**, 101101 (2014).
[7]A. J. Perry, J. N. Hodges, C. R. Markus, G. S. Kocheril, and B. J. McCall, J. Mol. Spectrosc. **317**, 71 (2015).
[8]C. R. Markus, J. N. Hodges, A. J. Perry, G. S. Kocheril, H. S. P. Müller, and B. J. McCall, Astrophys. J. **817**, 138 (2016).
[9]D. N. Gresh, K. C. Cossel, Y. Zhou, J. Ye, and E. A. Cornell, J. Mol. Spectrosc. **319**, 1 (2016).
[10]C. Savage, A. J. Apponi, and L. M. Ziurys, Astrophys. J. **608**, L73 (2004).
[11]D. T. Halfen and L. M. Ziurys, J. Mol. Spectrosc. **234**, 34 (2005).
[12]D. T. Halfen and L. M. Ziurys, Chem. Phys. Lett. **496**, 8 (2010).
[13]J. W. Farley, J. Chem. Phys. **95**, 5590 (1991).
[14]E. A. Mason and E. W. McDaniel, *Transport Properties of Ions in Gases* (John Wiley & Sons, New York, 1988).
[15]P. Kluczynski, J. Gustafsson, Å. M. Lindberg, and O. Axner, Spectrochim. Acta B **56**, 1277 (2001).
[16]H. Gao, Y.-Y. Liu, J.-L. Lin, J. Shi, G.-G. Xiong, Z.-H. Zhang, and D.-C. Tian, Acta Phys. Sin. **50**, 1463 (2001).
[17]S. Civiš, Chem. Phys. **186**, 63 (1994).
[18]P. Thompson, D. E. Cox, and J. B. Hastings, J. Appl. Crystallogr. **20**, 79 (1987).
[19]B. J. McCall, "Spectroscopy of H_3^+ in Laboratory and Astrophysical Plasmas," Ph.D. thesis, University of Chicago, 2001.
[20]K. N. Crabtree, J. N. Hodges, B. M. Siller, A. J. Perry, J. E. Kelly, P. A. Jenkins II, and B. J. McCall, Chem. Phys. Lett. **551**, 1 (2012).
[21]T. Ida, M. Ando, and H. Toraya, J. Appl. Crystallogr. **33**, 1311 (2000).
[22]A. von Engel, *Ionized Gases* (AIP Press, New York, 1965).
[23]B. M. Siller, J. N. Hodges, A. J. Perry, and B. J. McCall, J. Phys. Chem. A **117**, 10034 (2013).
[24]J. C. Pearson, L. C. Oesterling, E. Herbst, and F. C. De Lucia, Phys. Rev. Lett. **75**, 2940 (1995).
[25]F. F. Chen, *Introduction to Plasma Physics* (Plenum Press, New York, 1974).
[26]T. Oka, Phys. Rev. Lett. **45**, 531 (1980).
[27]T. N. Olney, N. Cann, G. Cooper, and C. Brion, Chem. Phys. **223**, 59 (1997).
[28]P. Neves, J. Escada, F. Borges, L. Tavora, and C. Conde, *IEEE Nuclear Science Symposium Conference Record* (IEEE, 2011), pp. 1793–1794.